Kinetic Considerations on the Olivine Cathodes

Assit. Prof. Atsuo Yamada

(Tokyo Institute of Technology)

Kinetic Considerations on the Olivine Cathodes

Atsuo Yamada*, Masao Yonemura, Yuki Takei, Noriyuki Sonoyama, and Ryoji Kanno

Department of Electronic Chemistry, Interdisciprinary Graduate School of Science and Engineering, Tokyo Institute of Technology
4259 Nagatsuta, Midori, Yokohama, 226-8502 Japan

Abstract

The electrochemical activity of the olivine type $LiMPO_4$ (M=transition metals) cathodes strongly depends on various factors, e.g., the transition metal element M, perturbative doping of the supervalent cations into Li site, composite formation with conductive additives, state of charge/discharge, and particle size and its geometries, etc. This is, therefore, an important issue of interdisciplinary between electrochemistry and solid state science towards practical applications. In order to shed light on this interesting but complicated issue with the transport properties and crystallographic aspects, systematic discussion will be made with the review of our recent publications; (1) first principle derivation of the electronic structures, (2) crystallographic mapping of the selected solid solutions, (3) quantitative elucidation of the electron-lattice interaction, (4) spectroscopic detection of the local environment with Mössbauer and EXAFS, (5) synthetic optimization of the electrode composite, and (6) electrochemical evaluation of the reaction kinetics, particularly on M = Fe, Mn.

Introduction

Lithium iron phosphate with ordered olivine structure, $LiFePO_4$, has now undoubtedly established its position as a next generation cathode material for lithium batteries with great advantages in terms of materials cost, chemical stability, and extreme safety but with no significant expense to the high energy density of the present materials such as $LiCoO_2$, $LiNiO_2$, and $LiMn_2O_4$[1-3]. This welcome boost was delivered by the Padhi et al.'s original report in 1997, where they have first demonstrated the electrochemical activity of Fe^{3+}/Fe^{2+} at 3.4V vs. Li/Li^+ in the ordered olivine structure, based on the two-phase reaction $LiFePO_4 \leftrightarrow FePO_4 + Li^+ + e^-$ with the first-order phase transition[1]. The redox potential of 3.4V is abnormally high close to that of bare Fe ions, 3.8V vs. Li/Li+, due to the large electronegativity of the $(PO_4)^{3-}$ polyanion which localizes the mobile electrons at the transition metal sites. The poor rate capability has been, therefore, attributed to slow diffusion of lithium ions across the two-phase boundary and/or low electronic conductivity, while the motional energy of lithium ions along the one-dimensional tunnel is calculated to be small[4]. To combat this issue, the extensive technical efforts have been directed to form smaller particles as well as to coat them with conductive media like carbon[3,5-12]. Another approach was made by Chiang et al. in order to enhance the bulk conductivity of $LiFePO_4$ by introducing a perturbative amount of supervalent cation M into the Li site together with the point defects $\square_a$ with a general chemical formula, $Li_{1-a-x}\square_a M^{b+}{}_x[Fe^{2+}{}_{1-(a-(b-1)x)}Fe^{3+}{}_{a-(b-1)x}]PO_4$, to form $Fe^{3+/2+}$ mixed valence state in both elements in two-phase redox reaction[13,14].

The position of M^{3+}/M^{2+} redox couple in $LiM(PO_4)^{3-}$ ordered-olivine family (Fe^{3+}/Fe^{2+}:3.4V[1], Mn^{3+}/Mn^{2+}:4.1V[1], Co^{3+}/Co^{2+}:4.8V[15]) can be well described in analogy with the inverse spinels $LiM(VO_4)^{3-}$ and trifluorides $Li_xM(F^-)_3$ system[16,17]. In terms of the electronegativity, $(PO_4)^{3-}$ shows greater acidity than that of $(VO_4)^{3-}$ with uniformly higher voltages by ca. 0.6 V, whereas $(F^-)_3$ shows intermediate both in acidity and redox potentials. These systematic inductive effects are summarized in Fig. 1. In general, the higher ionic nature of the transition metal M leads to the higher voltage cathode sacrificing the electrochemical activity by the electron localization.

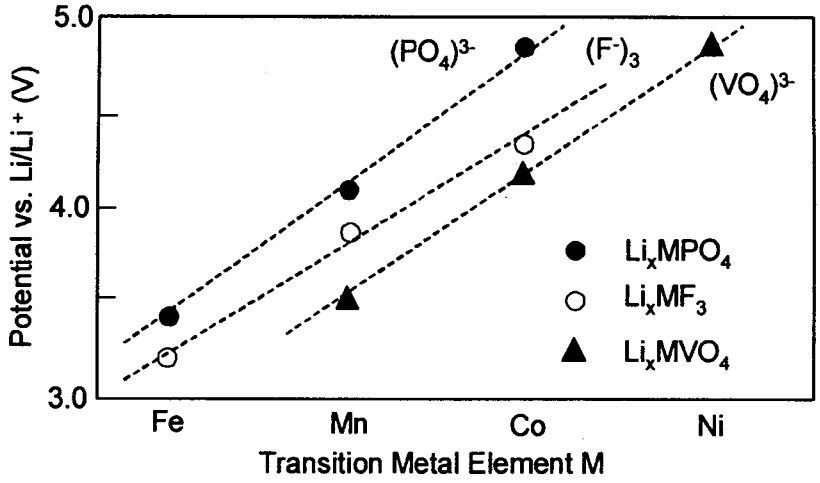

Fig. 1 Systematic inductive effects in Li_xMPO_4, Li_xMF_3, and Li_xMVO_4

The drastic improvement of the cathode activity of $LiFePO_4$ has initiated the motivation that some other ionic insulating compounds may be nominated as a novel promising material for lithium battery cathode, and naturally led many researchers to apply the same strategy to other transition metal olivines[18-23], transition metal trifluorides[24,25], and different form of transition metal phosphates[23-28]. Among them, it is interesting to note that the recent studies on FeF_3/C nanocomposite have shown, in addition to the enhanced Fe^{3+}/Fe^{2+} topotactic electrochemical activity, reversible decomposition into Fe nanometric metal cluster dispersed in LiF matrix at lower voltage region[24,25], as earlier observed in metal oxide nanoparticles[31]. Recently, the importance of the concept "reversible nano-decomposition" has also been recognized as the novel strategy for hydrogen storage materials as demonstrated in metal alanates[32-34] and metal nitrides[35,36]. It is also noteworthy that, in Padhi et al.'s original paper1, they addressed the position of Mn^{3+}/Mn^{2+} redox couple in ordered olivine framework at 4.1V vs. Li/Li^+, and its electrochemical activity has been significantly improved in the later publications with systematic identification of the reaction mechanisms[18-21]. Intuitively, the higher open circuit voltage within the electrolyte stability window would lead to a practical cathode with higher energy density. Indeed, there was an argument which addressed the promising perspectives for $LiMnPO_4$ as superior candidate to $LiFePO_4$ for a practical lithium battery cathode[22].

Experimental difficulties, however, in evaluating the electrochemical activity of these inherently insulating compounds lie in the fact that the cathode performance, especially current durability, strongly depends on the many extrinsic factors, such as particle size, structure of carbon additive, the amount of carbon additive, mixing and sintering recipe, the electrode thickness, the cell configurations, and so on. It is this situation that has often led many battery engineers into a puzzle with poor reproducibility of the published data in an actual cell. This, in turn, is suggestive that the data can be modified as it looks like promising under the unrealistic experimental conditions, e. g., very low current density <C/20 at elevated temperatures, very thin electrode film with $< \sim 10\mu m$ thickness, electrode composite with very low tap-density by using nano-particles and/or large amount of carbon to coat them, etc., many of which have not been appropriately mentioned in the literatures so far. Cautions for such extrinsic experimental tricks were timely made by Chen and Dahn[10], and also by Doeff et al[37].

In this paper, careful electrochemical measurements are performed under the reasonable and identical extrinsic conditions to shed light on the huge kinetic difference of Li_xFePO_4 and Li_xMnPO_4 in a quantitative manner, followed by the comparative discussions based on their intrinsic difference in crystallographic aspects and transport properties.

Experimental

Self assembled $LiMPO_4$ (M = Fe, Mn) / carbon composites were synthesized based on the carbon coating concept first proposed by Ravet et al.[5], and the recipe was a modification of those described in ref. 6 and ref. 12. Stoichiometric amounts of Li_2CO_3 (lithium carbonate, Wako, >99.9 % purity), $(NH_4)_2HPO_4$ (hydrogen ammonium phosphate, Wako, >99.9 % purity), $Fe(II)C_2O_4.2H_2O$ (iron oxalate dihydrate, Aldrich, >99 % purity), and $Mn(II)C_2O_4.0.5H_2O$ (manganese oxalate hemihydrate, Wako, >99 % purity) were used as starting materials. The ketjenblack was added with an estimated amount in the final $LiMPO_4$/C composite to be 10 wt%[12]. The mixture was homogenized and reground by high-energy planetary ballmilling for 6 hours, followed by a sintering in a pellet form at 600C for 6 hours under a flow of purified Ar gas.

X-ray diffraction patterns of the powdered samples were obtained with an X-ray diffractometer (Rigaku TAD-C, 12kW) with Cu-Kα radiation. The diffraction data were collected at each 0.02 step width over a 2θ range from 10° to 100°. The structural parameters were refined by Rietveld analysis using the computer program RIETAN 2000. The particle texture was observed by scanning electron microscopy (SEM, Hitachi S-4000). The Brunauer, Emmett, and Teller (BET) method was used to measure the surface area of powders (Coulter, SA-3100). To measure the tap density, about 2 g of sample powder was placed in a 5 ml cylinder and tapped on the lab. bench several times. The measured volume of the tapped powder was used to calculate the tap density.

The electrochemical measurements were performed with a stainless steel cell (HS test cell, Hosen Co.) with the electrolyte of 1M solution of LiPF6 in 7:3 ethylene carbonate / diethyl carbonate (EC/DEC) (Mitsubishi Petrochemical, battery grade). The counter electrode was a 15mm diameter and 0.30mm thickness disk of lithium metal foil. The separator employed was a glass filter sheet. The working electrode was a mixture of cathode composite / polyvinylidene fluoride (PVDF) with 10:1 weight ratio. The mixture was added to the minimum amount of N-methylpyrrolidon (NMP), and the slurry was cast on Al film. After drying at 120°C, it was punched into a circular disk. The active materials layer was 70mm thickness with ca. 10mg/cm2, both of them are in the reasonable ranges as an electrode for the practical lithium battery.

All electrochemical tests were performed at 25°C. Kinetic differences were measured galvanostatically for a cathodic direction. After the full charging by slow rates (C/100 for $LiMnPO_4$ or C/20 for $LiFePO_4$) to 4.5 V followed by the constant voltage mode with a cut-off current density of C/1000 rate, the cell was discharged at different specified current rates ranging from C/100 to 10C.

Results and Discussion

The X-ray diffraction profiles for $LiMPO_4$ / C (M = Fe, Mn) composites were refined, where the internal carbon could be treated as a contribution to the background. Initial coordinates for $LiMPO_4$ with space group Pnma were Li at 4a (0, 0, 0), Fe at 4c (x, 1/4, z) with x ~ 0.28 and z ~ 0.97, P at 4c (x, 1/4, z) with x ~ 0.10 and z ~ 0.42, O1 at 4c (x, 1/4, z) with x ~ 0.10 and z ~ 0.74, O2 at 4c (x, 1/4, z) with x ~0.45 and z ~ 0.20, and O3 at 8d (x, y, z) with x ~ 0.16, y ~ 0.05, and z ~ 0.28. Although several types of cation disorder and vacancy modes were considered for refinements, both of $LiFePO_4$ and $LiMnPO_4$ were refined to be the stoichiometric compositions. The superimposed, observed, and calculated X-ray diffraction profiles are shown in Fig. 1, and the refined results are summarized in the table. The average particle size was estimated to be 95.7 nm and 79.1 nm for $LiFePO_4$ and $LiMnPO_4$, respectively, using the conventional Scherrer equation.

SEM images of $LiFePO_4$/C and $LiMnPO_4$/C composites showed the aggregates with different sizes were observed for both samples, but the primary particles are of almost the same size and morphology. Typical particle sizes in the range of 60 nm ~ 100 nm are consistent with the Scherrer's particle diameter obtained by the Reitveld refinement of the XRD data. Reasonably, the BET surface area measured to be almost the same, 55.02 m^2/g for $LiFePO_4$/C and 55.84 m^2/g for $LiMnPO_4$/C. The tap density (ρ_T) also showed almost identical values of 0.89 g/cm3 and 0.84 g/cm3 for $LiFePO_4$/C and $LiMnPO_4$/C composites, respectively. The small difference can be explained by the smaller crystalline density (ρ_C) of $LiMnPO_4$ (3.4g/cc) than that of $LiFePO_4$ (3.6g/cc).

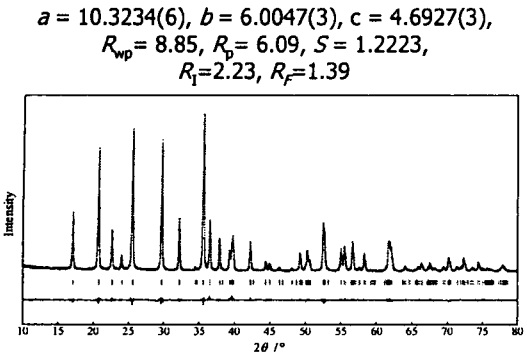

Atom	site	g	x	y	z	B (Å²)
Li	4a	1	0	0	0	1
Fe	4c	1	0.28223(12)	1/4	0.974(4)	0.6
P	4c	1	0.0955(2)	1/4	0.4177(5)	0.6
O(1)	4c	1	0.09489(6)	1/4	0.7440(12)	1
O(2)	4c	1	0.4565(7)	1/4	0.2074(11)	1
O(3)	8d	1	0.1661(5)	0.0472(7)	0.2835(7)	1

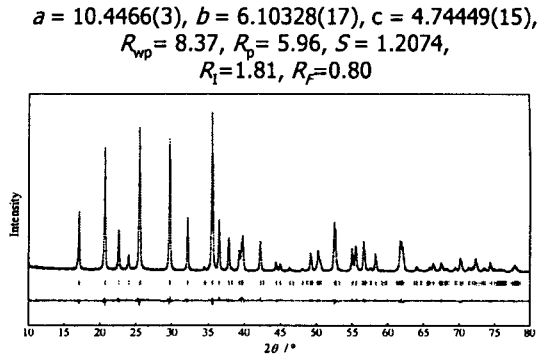

Atom	site	g	x	y	z	B (Å²)
Li	4a	1	0	0	0	1
Mn	4c	1	0.28145(10)	1/4	0.9705(4)	0.6
P	4c	1	0.0928(2)	1/4	0.4087(5)	0.6
O(1)	4c	1	0.0940(6)	1/4	0.7328(11)	1
O(2)	4c	1	0.4563(6)	1/4	0.2167(9)	1
O(3)	8d	1	0.1623(4)	0.0520(6)	0.2777(7)	1

Fig. 2 Rietveld refinement patterns of $LiFePO_4$/C (left) and $LiMnPO_4$/C (right) for the X-ray diffraction data taken at room temperature. The observed intensity data are shown by dots, and the solid line overlying them is the calculated intensity. Vertical markers below the diffraction patterns indicate positions of possible Bragg reflections. Differences between the observed and calculated intensities are plotted as Dyi at the bottom in the same scale.

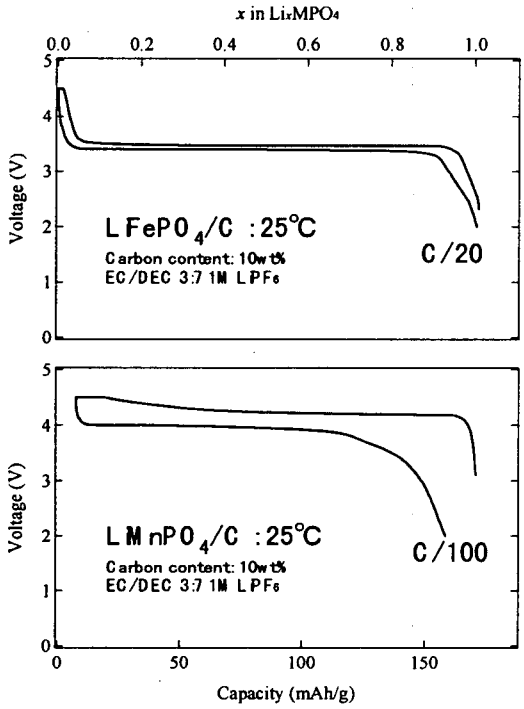

Fig. 3 Galvanostatic charge-discharge profiles measured at 25°C for (a) $LiFePO_4$/C at C/20 rate and (b) $LiMnPO_4$/C at C/100 rate.

Anyhow, under these controlled identical extrinsic conditions for the electrode composites, the following comparative electrochemical tests with identical cell configurations should reveal the intrinsic kinetic differences of Li_xFePO_4 and Li_xMnPO_4, which is one of the major subjects of this paper.

Figure 3 (b) shows the trickle galvanostatic charge-discharge curves of Li_xMnPO_4 measured at C/100 rate. Under such a slow rate condition, $LiMnPO_4$ show large capacity with modest polarization. This looks somewhat consistent with the previous report[19] that high capacity can be delivered from $LiMnPO_4$ without any intrinsic obstacles when the optimized synthetic method [6,12] is applied to form an electrode composite with carbon. However, abnormally slow rate of C/100 corresponds to ~ 1 week charge and ~ 1week discharge and is apparently not in a realistic condition. Furthermore, even in such a very slow rate, large polarization in Li_xMnPO_4 is evident both at the end of charge and discharge, and hence the theoretical capacity can not be reached with significant irreversible loss; C/100 – C/1000 is not slow enough for $LiMnPO_4$. On the other hand, the capacity of $LiFePO_4$ reached exactly to the theoretical value both for charge and discharge with negligible polarization even at much higher current rate of C/20, as shown in Fig. 3(a).

At higher current rate conditions, the kinetic difference became much more obvious. Figure 4 shows the discharge curves at different specified current rates after the full charging process. During the discharge process of Li_xMnPO_4 at >C/20 rates, it is hardly identify the flat 4V region, and quickly suffered from very large polarization as have mentioned in the previous literature[1,18,20]. As a consequence, the capacity decrease is precipitous with increase of current density. For Li_xFePO_4, on the other hand, the voltage plateau is maintained against relatively higher current density over 1C rate, where more than 80% of its theoretical capacity is still obtained.

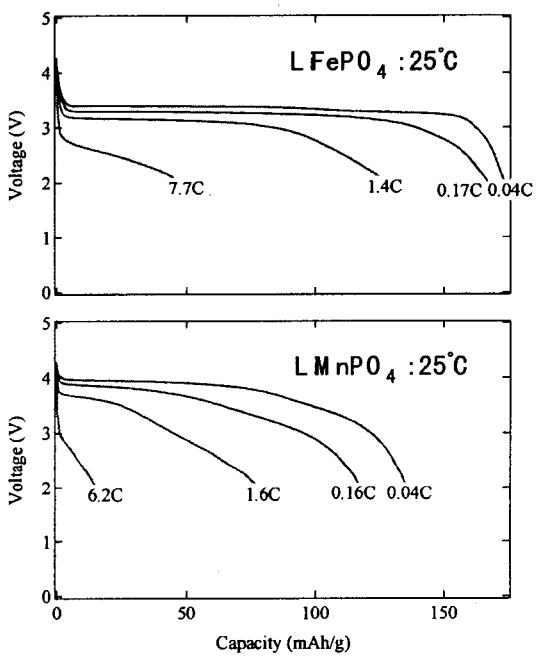

Fig. 4 The discharge curves measured at 25°C for (a) $LiFePO_4$/C and (b) $LiMnPO_4$/C at different specified current rates after the sufficiently trickle full charging process.

As a summary of these results, the effective volumetric energy density is plotted in Fig. 5 as a function of the discharge current rates. For a convenience, times required for utilizing full capacity are also denoted. The two transverse dotted lines are the ideal energy densities based on the theoretical capacities and the open circuit voltages, and of course $LiMnPO_4$ shows a higher value. However, under the realistic kinetic situations, the energy density of $LiMnPO_4$ is always much lower than that of $LiFePO_4$. Usually, the minimum requirement in current durability for lithium-ion batteries is >0.5C and in most cases >1C. The kinetic difference is actually very large because the current rate in Fig. 5 is plotted in a logarithmic scale. Indeed, Fig. 5 covers the very wide range of time scale from 6 minutes to 3 months. For instance, in order to achieve the same energy density as large as $LiFePO_4$, only less than one tenth of the current can be allowed to $LiMnPO_4$. With a simple line extrapolation, $LiMnPO_4$ will exceed the energy density of $LiFePO_4$ at 10 days rate, and reaches its theoretical energy density at 1 month discharge rate. Nevertheless, battery design for one month operation is in most cases unrealistic. Consequently, it is reasonable to conclude that the effective energy density of $LiMnPO_4$ is much lower than that of $LiFePO_4$. The intuitive energy density estimation just based on the open circuit voltage is quite misleading.

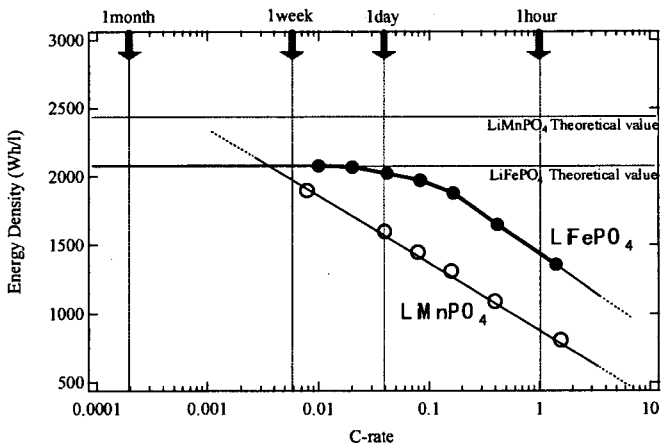

Fig. 5 Comparative representation of the "effective" volumetric energy density of $LiFePO_4$ and $LiMnPO_4$ as a function of the discharge current rate.

To our knowledge, this is the first report on the systematic quantitative presentation of the kinetic difference in Fe^{3+}/Fe^{2+} and Mn^{3+}/Mn^{2+} redox reactions in the olivine framework, though the large polarization and/or limited capacity for Li_xMnPO_4 has been reported in the previous literatures[1,18,20]. Since the comparative experiments in this study were performed under the identical extrinsic conditions, the huge kinetic difference is clearly associated with the intrinsic aspects of solids. Although the sophisticated synthetic recipe may somewhat improve the reaction kinetics, there should be always large relative kinetic differences coming from the intrinsic properties dominating the overall trend. This is the reason why the optimistic perspectives for pure $LiMnPO_4$ as practical cathode have not been widely accepted in the community and is also out of consideration in our policy. Abnormally low rate capability of intrinsic nature, especially at the charging process, significantly limits the practical application area.

Indeed, these arguments have been supported by the most of the previous theoretical and experimental works. Many descriptions on the difference of the intrinsic properties can be found in the previous literatures with an eye to the crystallographic aspects and transport properties[38], particularly on those associated with the Jahn-Teller effect of Mn^{3+} ions[18]. The large effective mass of the polaronic holes around Mn^{3+} ions coupled with large local lattice deformations[20] has been suggested to induce the slow kinetics[19] and the internal friction either in bulk crystal or at the $LiMnPO_4/MnPO_4$ two-phase interface, as evidenced by significant crystallinity loss and/or local phase segregation[18].

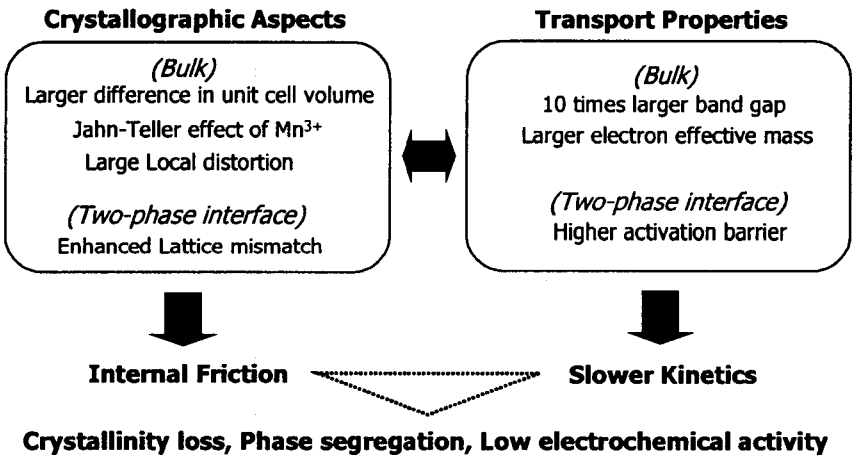

Fig. 6 Mapping possible reasons for low electrochemical activity of Mn^{3+}/Mn^{2+} redox couple in olivine framework.

More generally, we should be aware of that the most of the electrode materials, including the future candidates under research, are metal or semiconductor at room temperature with conductivity $>10^{-4}$S/cm, while the inherently insulating $LiFePO_4$ with ~10^{-8} S/cm is already an exceptionally rare case[39] (Fig. 7). As for Li_xMnPO_4, the electrons/holes are probably much more localized not only in the trivalent state ($Mn^{3+}PO_4$) but also in divalent state ($LiMn^{2+}PO_4$). For instance, our preliminary four-probe measurement revealed that $LiMnPO_4$ is a severe insulator with very low conductivity which is out of the measurement range ($<10^{-10}$S/cm), and may be consistent with the large spin-exchange gap of 3 eV, which is one-order larger than the 0.15eV crystal field gap of $LiFePO_4$[18] (Fig. 8), and/or the longer hopping distance of polarons for Mn-O-Mn linkage than that for Fe-O-Fe; the unit cell volume of $LiMnPO_4$ (303.3 Å^3) is larger than that of $LiFePO_4$ (291.2 Å^3)[1,18]. These several intrinsic frustrations for the smooth cathode reaction are much enhanced at the higher rate conditions. Although further study is still necessary to address the dominant rate-limiting factor, our recent electrochemical study strongly suggest the heavy polaronic holes around Mn^{3+} play a very important role, and will be published in the future publications[40].

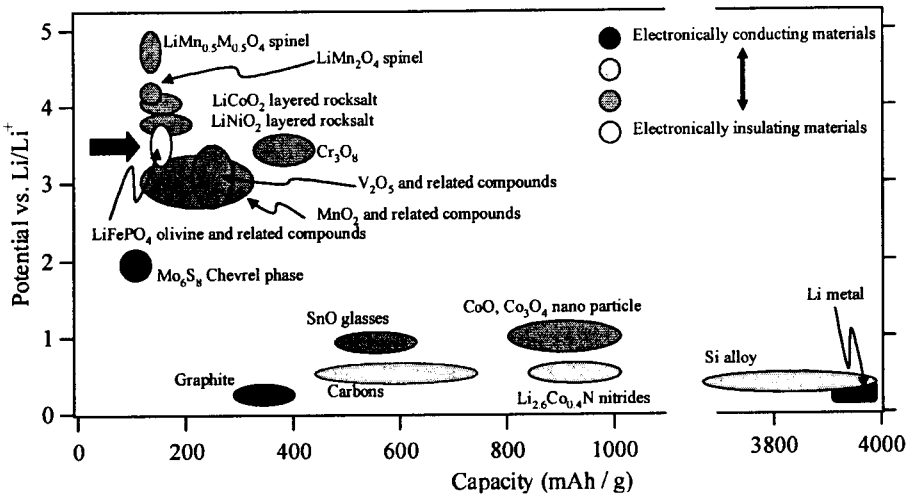

Fig. 7 Relationship between the potential and the capacity for the electrode materials together with the information on the electronic conductivity.

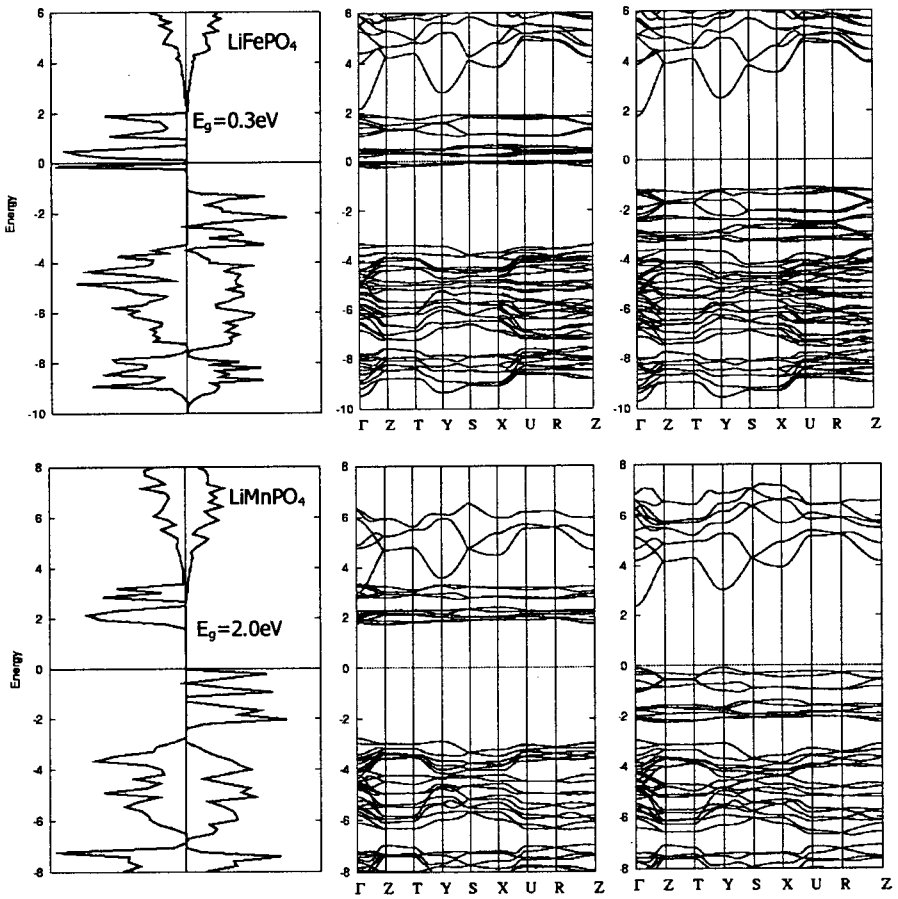

Fig. 8 Total density of states and band dispersion of $LiFePO_4$ and $LiMnPO_4$

Conclusions

Even though the recent progresses on the nano-coating technologies have opened the door to screen hitherto unexplored insulator for lithium battery cathodes, $LiFePO_4$ still hold its great advantages so far with respect to (1) moderate electrochemical activity with flat voltage profile at 3.4V at reasonable current rates, (2) wide voltage margin against the oxidative electrolyte decomposition without significant loss of energy density, (3) extremely low material cost, (4) low toxicity, (5) initial lithium durability for the carbon anode, (5) extreme safety and stability, and (6) reasonably high volume density (3.6g/cc) with HCP oxygen sub-array. Particularly, the factor (2) looks very convenient for a quick charging and stable long-term operations. One should not be overly optimistic to all insulating ionic compounds for practical applications without sufficient considerations on their materials intrinsic properties, which essentially dominates the overall trend of the electrochemical activity. As a typical example for this, it is demonstrated in a quantitative manner that the electrochemical activity of the Mn^{3+}/Mn^{2+} redox reaction in the olivine framework of Li_xMPO_4 (M = transition metals) is extremely lower than that of Fe^{3+}/Fe^{2+}, and the large difference in current durability by more than order of magnitude is not in an acceptable level to serve as a practical lithium battery cathode. There is no ambiguity that the huge kinetic difference is associated with the materials intrinsic properties and the heavy polarons around Mn^{3+} are suggested as an important rate-limiting factor. As a consequence, the effective energy density of $LiMnPO_4$ as a lithium battery cathode is much lower than that of $LiFePO_4$ in spite of the inherent higher open circuit voltage.

References

1. A. K. Padhi, K. S. Nanjundaswamy, and J. B. Goodenough, *J. Electrochem. Soc.*, 144, 1188 (1997)
2. J. M. Tarascon and M. Armand, *Nature*, 415, 359 (2002)
3. A. Yamada, S. C. Chung, and K. Hinokuma, *J. Electrochem. Soc.*, 148, A224 (2001)
4. D. Morgan, A. van der Ven, and G. Ceder, *Electrochem. Solid State Lett.*, 7, in press (2004)
5. N. Ravet, J. B. Goodenough, S. Besner, M. Simoneau, P. Hovington, and M. Armand, Abstract 127, *The Electrochemical Society and the Electrochemical Society of Japan Meeting Abstracts*, Vol. 99-2, Honolulu, HI, Oct 17-22, (1999)
6. A. Yamada, M. Hosoya, S. C. Chung, Y. Kudo, and K. Y. Liu, *Proc. Electrochem. Soc. Meeting*, PV-2001-21, 149 (2001)
7. P. P. Prosini, D. Zane, and M. Pasquali, *Electrochim. Acta*, 46, 3517 (2001)
8. S. Yang, P. Y. Zavalij, and M. S. Whittingham, *Electrochem. Commun.*, 3, 505 (2001)
9. H. Huang, S.-C. Yin, and L. F. Nazar, *Electrochem. Solid State Lett.*, 4, A170 (2001)
10. Z. Chen and J. R. Dahn, *J. Electrochem. Soc.*, 149, A1184 (2002)
11. S. Franger, F. Le Cras, C. Bourbon, and H. Rouault, *Electrochem. Solid State Lett.*, 5, A231 (2002)
12. A. Yamada, M. Hosoya, S. C. Chung, Y. Kudo, K. Hinokuma, K. Y. Liu, and Y. Nishi, *J. Power Sources*, 191-121, 232 (2003)
13. S. Y. Chung, J. T. Bloking, and Y. M. Chiang, *Nature Mater.*, 2, 123 (2002)
14. S. Y. Chung and Y. M. Chiang, *Electrochem. Solid State Lett.*, 6, A278 (2003)
15. K. Amine, H. Yasuda, and M. Yamachi, *Electrochem. Solid State Lett.*, 3, 178 (2000)
16. A. K. Padhi, W. B. Archibald, K. S. Nanjundaswamy, and J. B. Goodenough, *J. Solid State Chem.*, 128, 267 (1997)
17. H. Arai, S. Okada, Y. Sakurai, and J. Yamaki, *J. Power Sources*, 68, 716 (1997)
18. A. Yamada and S. C. Chung, *J. Electrochem. Soc.*, 148, A960 (2001)
19. A. Yamada, Y. Kudo, and K. Y. Liu, *J. Electrochem. Soc.*, 148, A747 (2001)
20. A. Yamada, Y. Kudo, and K.Y. Liu, *J. Electrochem. Soc.*, 148, A1153 (2001)
21. A. Yamada, M. Hosoya, S. C. Chung, K. Hinokuma, Y. Kudo, and K. Y. Liu, *Ceram. Trans.*, 127, 189 (2002)

22. G. Li, H. Azuma, and M. Tohda, *Electrochem. Solid State Lett.*, 5, A960 (2002)
23. M. Lloris, C. P. Vicente, J. L. Tirado, *Electrochem. Solid State Lett.*, 5, A234 (2002)
24. F. Badway, N. Pereira, F. Cosandey, G. G. Amatucci, *J. Electrochem. Soc,* 150, A1209 (2003)
25. F. Badway, F. Cosandey, N. Pereira, and G. G. Amatucci, *J. Electrochem. Soc,* 150, A1318 (2003)
26. M. Y. Saïdi, J. Barker, H. Huang, J. L. Swoyer, and G. Adamson, *Electrochem. Solid State Lett.*, 5, A149 (2002)
27. H. Huang, S. C. Yin, T. Kerr, N. Taylor, L. F. Nazar, *Adv. Mater.*, 14, 1525 (2002)
28. D. Morgan, G. Ceder, M. Y. Saidi, J. Barker, J. Swoyer, H. Huang, G. Adamson,, *Chem. Mater,* 14, 4684 (2002)
29. C. Masquelier, P. Reale, C. Wurm, M. Morcrette, L. Dupont, and D. Larcher, *J. Electrochem. Soc.*, 149, A1037 (2002)
30. Y. Song, P. Y. Zavalij, M. Suzuki, and M. S. Whittingham, *Inorg. Chem.*, 41, 5778 (2002)
31. P. Poizot, S. Laruelle, S. Grugeon, L. Dupont, and J. M. Tarascon, *Nature*, 407, 496 (2000)
32. B. Bogdanovic, M. Schwickardi, *J. Alloys and Comp.*, 253, 1 (1997)
33. H. Morioka, K. Kakizaki, S. C. Chung, and A. Yamada, *J. Alloys and Comp.*, 353, 310 (2003)
34. M. E. Arroyo y Dompablo and G. Ceder, *J. Alloys and Comp.*, in press (2004)
35. P. Chen, Z. Xiong, J. Luo, J. Lin, and K. L. Tan, *Nature*, 420, 302 (2002)
36. T. Ichikawa, S. Isobe, N. Hanada, H. Fujii, *J. Alloys and Comp.*, in press (2004)
37. M. M. Doeff, Y. Hu, F. McLarnon, R. Kostecki, *Electochem. Solid State Lett.*, 6, A207 (2003)
38. A. Yamada, M. Yonemura, Y. Takei, N. Sonoyama, and R. Kanno, Abstract Inv. 3, Lithium Battery Discussion – Electrode Materials, Arcachon, France, Sept. 14-19, (2003)
39. R. Kanno, *Electrochemistry,* 71, 710 (2003)
40. M. Yonemura, A. Yamada, Y. Takei, N. Sonoyama, and R. Kanno, to be published.